



HAL
open science

Corrosion of rebars embedded in ancient concrete: correlation between on site testing and corrosion products identification

Elisabeth Marie Victoire, Emmanuel Cailleux, Delphine D. Neff, Valérie L'Hostis, E Marie Victoire, Laurent Vincent, Annick Texier, Ludovic Bellot-Gurlet, Philippe Dillmann

► **To cite this version:**

Elisabeth Marie Victoire, Emmanuel Cailleux, Delphine D. Neff, Valérie L'Hostis, E Marie Victoire, et al.. Corrosion of rebars embedded in ancient concrete: correlation between on site testing and corrosion products identification. 11, Istanbul Technical University, pp.T71_1-9, 2008. hal-02133524

HAL Id: hal-02133524

<https://hal.science/hal-02133524v1>

Submitted on 18 May 2019

HAL is a multi-disciplinary open access archive for the deposit and dissemination of scientific research documents, whether they are published or not. The documents may come from teaching and research institutions in France or abroad, or from public or private research centers.

L'archive ouverte pluridisciplinaire **HAL**, est destinée au dépôt et à la diffusion de documents scientifiques de niveau recherche, publiés ou non, émanant des établissements d'enseignement et de recherche français ou étrangers, des laboratoires publics ou privés.

Corrosion of Rebars Embedded in Ancient Concrete : Correlation between on Site Testing and Corrosion Products Identification

E. Marie Victoire¹

E. Cailleux²

D. Neff³

V. L'Hostis⁴

L. Vincent⁴

A. Texier¹

L. Bellot-Gurlet⁵

P. Dillmann⁶

T 71

ABSTRACT

Several hundreds of buildings made of reinforced concrete are now classified as historical in France. Their major pathology is carbonation induced corrosion. The cracking and spalling decays induced by this natural aging process cause loss of material incompatible with the deontology of historical monuments conservation. Therefore it is crucial to understand the corrosion process of embedded steel and to be able to evaluate precisely the corrosion activity on site, in order to predict and may-be to prevent such decays. Current on site non destructive tools for diagnosis operations are potential mapping or corrosion rate measurements. But, such electrochemical techniques are clearly season influenced. Moreover, corrosion rates induced by carbonation are often very low and therefore can be difficult to measure. As a consequence, in areas heavily affected by spalling phenomena, low corrosion activity is often evidenced, so that the interpretation of the results can be problematic. A last hypothesis could be that the oxide layer formed is so resistive that the conductivity necessary for the measurement is lost. In order to better understand the corrosion process of rebars embedded in carbonated concrete, and may be to improve the reliability of those diagnosis tools, it seemed interesting to try to correlate on site measurements with the identification of corrosion patterns. Therefore, on a 56 years old industrial building (Air Purifier of the Meudon Wind tunnel), several sets of potential mapping, resistivity and corrosion rate measurements were performed, respectively in winter time and in spring time, and after medium or heavy moistening. Then reinforced concrete cores were sampled both in supposed active and passive corrosion areas, in order to evaluate the carbonation depth and to identify the corrosion patterns.

KEYWORDS

Historical buildings, Concrete, Corrosion, Diagnosis tool, Corrosion patterns

¹ Laboratoire de Recherche des Monuments Historiques, Champs-sur-Marne, France, Phone 33 1 60 37 77 84, Fax 33 1 60 37 77 99, annick.texier@culture.gouv.fr

² Cercle des Partenaires du Patrimoine, Champs-sur-Marne, Fr, Ph 33 1 60 377786, emmanuel.cailleux@culture.gouv.fr

³ Laboratoire Pierre Süe, CEA/CNRS UMR 9956, CEA Saclay, Gif-sur-Yvette, France, Phone 33 1 69 08 33 40, Delphine.neff@cea.fr

⁴ LECBA, CEA Saclay, 91191 Gif/Yvette cedex, France, Phone, Fax, valerie.lhostis@cea.fr, laurent.vincent@cea.fr

⁵ Laboratoire de Dynamique, Interaction et Réactivité (LADIR), UMR 7075 CNRS and Université Pierre et Marie Curie Paris 6, Thiais, France, Phone 33 1 49 78 11 14, Fax 33 1 49 78 11 18, Bellot-Gurlet@glvt-cnrs.fr

⁶ I RAMAT LMC CNRS UMR5060 & Laboratoire Pierre Süe CEA/CNRS UMR9956, CEA Saclay, Gif-sur-Yvette, France, Phone 33 1 69 08 14 69, Fax 33 1 69 08 69 23, philippe.dillmann@cea.fr

1 INTRODUCTION

One of the major sources of decay of historical monuments made of reinforced concrete in France is carbonation. This phenomenon consists in a reaction between atmospheric carbon dioxide and the cement paste hydrates, inducing a decrease of pH from values up to 13 in a sound concrete, down to 9 in a carbonated concrete. At these lower pH values, concrete is no longer protective for the steel reinforcement and an active corrosion of the rebars can take place if enough water and oxygen are available. Nevertheless, this corrosion process, very influenced by atmospheric conditions, seems slow-acting, and therefore it is sometimes difficult to monitor on site through electrochemical measurements. Moreover, in heavily decayed areas, where thick oxide layers can be observed, sometimes very low corrosion activities are measured. As a consequence, interpretation of on site measurements can be tricky. So it seemed interesting on one hand to study the influence of atmospheric conditions but also of preliminary moistening on electrochemical on site tests ; and on the other hand to verify these measurements by identifying the corrosion patterns on points prior assessed either active or passive.

2 TESTING SITE AND PROTOCOLE

2.1. Description and Preliminary Characterization

Tests were performed on the extension of a wind tunnel, built in 1950 in the western suburb of Paris (Figs 1 and 2). On the eastern façade, of this ancient air purifier, numerous honeycombing and spalling areas were visible on the pillars, with locally very thick oxides layers (Fig. 3). Due to the age of the building, a carbonation induced corrosion was suspected.

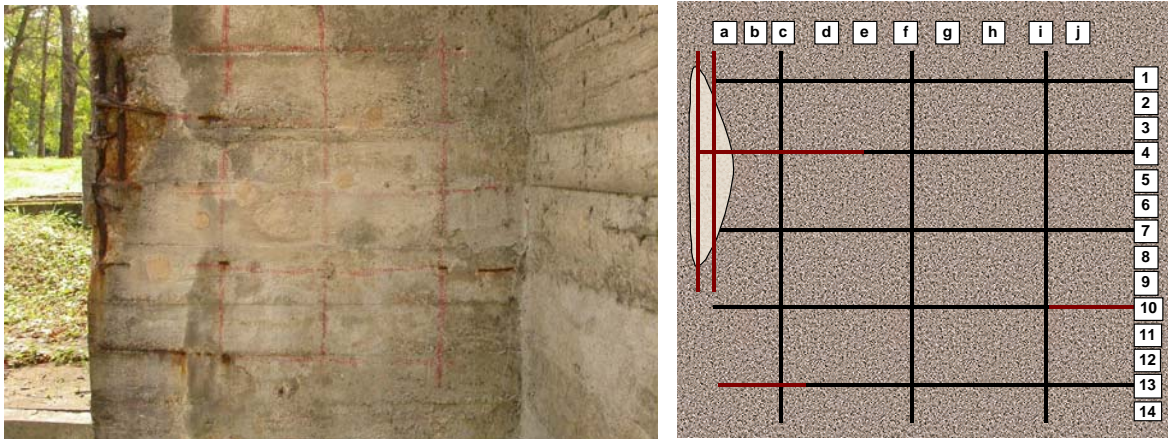


Figures 1, 2 and 3 : The air purifier (on the left) is an extension of the Meudon wind tunnel (in the center). It is locally very decayed, with large spalling areas (on the right) often linked to honeycombing.

In a prior study [1] characterization by optical and SEM observations of both fractures and cross sections revealed a great heterogeneity of the concrete ; locally very compact areas, with good cement-aggregates contacts, cohabiting with numerous very porous zones. A carbonation phenomenon was observed, portlandite being gradually replaced by calcite, but the extent of the reaction was clearly linked to the compactness of the concrete. Finally, cement was identified as an Ordinary Portland Cement containing small amounts of slag, which can be compared to a current CEM II/A.

2.2. Testing Area

A 1m² testing area, with a large spalling zone and visible corroded rebars was selected (Fig.4). In this testing zone, 5 vertical rebars (2 being visible) and 5 horizontal rebars were located (Fig.5) using an electromagnetic technique (pachometer rebar plus©).



Figures 4 and 5 : In the selected testing area (left picture), 5 vertical and 5 horizontal rebars were located (right diagram).

2.3. Testing protocole

First in order to evaluate the influence of the climate on the corrosion activity, a series of electrochemical measurements (resistivity, potential mapping and corrosion rate) was carried out on site, both in winter and in spring time, after standard moistening of the examined surface. Then to study the impact of preconditioning, during the spring tests, 2 sets of measurements were performed respectively after heavy moistening or after heavy and repeated moistening. Then, as carbonation was the suspected source of corrosion of the rebars, the carbonation depth was evaluated through phenolphthalein tests, realized on cores.

Finally, cores containing a rebar were sampled on areas identified by the electrochemical measurements as active or passive. From those cores, in order to identify the corrosion species, cross sections were prepared and optical microscopy, Scanning Electron Microscopy (SEM) coupled to Energy Dispersive Spectroscopy (EDS), and Raman micro-spectrometry were carried out following the protocole described by Neff & al. [8].

3 ON SITE TESTING

3.1. Resistivity Measurements

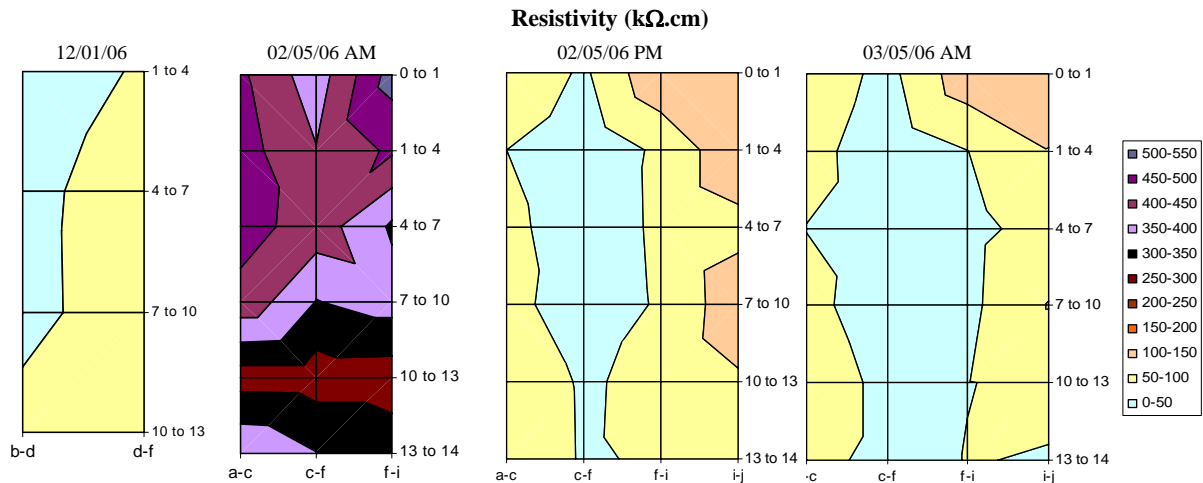
Resistivity measurements were performed with a Gecor6© device, using a copper-copper sulfate electrode. Four thresholds of corrosion risk are indicated by the manufacturer, from nil ($\rho > 100 \text{ k}\Omega\cdot\text{cm}$) to low ($50 < \rho < 100 \text{ k}\Omega\cdot\text{cm}$), moderate ($10 < \rho < 50 \text{ k}\Omega\cdot\text{cm}$), up to high ($\rho < 10 \text{ k}\Omega\cdot\text{cm}$). But in practice, such measurements which are so dependent on the concrete dampness and salts contents, are more used as a relevance indicator for electrochemical measurements. Thus, it is commonly admitted that when resistivity is higher than 100, the concrete is too dry, and when it is lower than 5, it is too water saturated, to perform electrochemical measurements.

In winter time (12/01/06, 5.2°C, 70% RH), resistivity values ranging between 9 and 30 were measured (Fig. 6), indicating a suitable moisture content for electrochemical measurements, with a moderate corrosion risk.

The first measurements performed in springtime (02/05/06 AM, 15.4°C, 53.3% RH, Fig. 7) after “standard” preliminary moistening, lead to resistivity values between 273 and 521 $\text{k}\Omega\cdot\text{cm}$, indicating that the concrete was clearly too dry.

After heavy moistening, a new series of measurements was carried out (02/05/06 PM, 18.5°C, 43.8% RH, Fig. 8), and resistivity values between 19 and 144 kΩ.cm were collected, indicating that the concrete was then wet enough for electrochemical measurements, even if the corrosion risk stayed moderate to low.

The day after, a last set of resistivity measurement was performed (03/05/07 PM, 19.7°C, 54.3% RH, Fig. 9), after heavy and repeated wetting of the testing area. Values very close to the previous ones, ranging between 10 and 133 kΩ.cm, were measured.



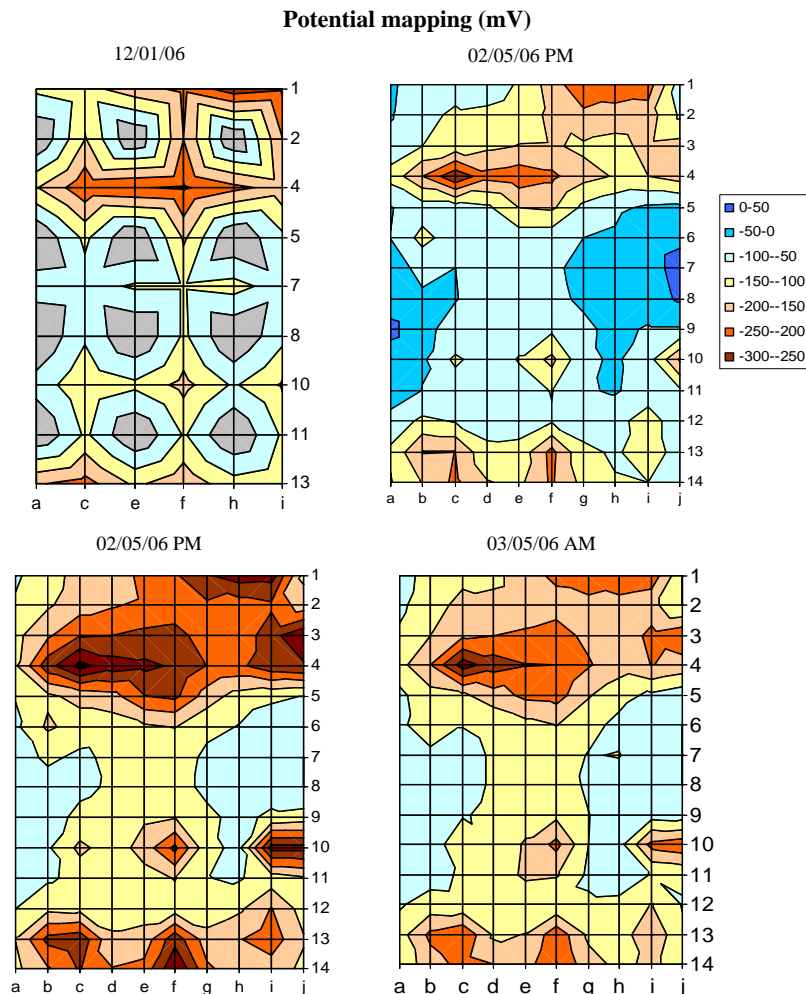
Figures 6, 7, 8 and 9 : Resistivity mapping realized in winter time (12/01/06) ; and in springtime after standard moistening (02/05/06 AM), after heavy moistening (02/05/06 PM), and after heavy and repeated moistening (03/05/06 AM).

3.2. Potential mapping

Potential mappings were carried out using a Canin© corrosimeter, equipped with a copper-copper sulfate reference electrode. If ASTM C876 standard defines thresholds of corrosion probability for potential measurements, it is commonly admitted that it is preferable to realize potential mapping and to identify potential gradients. Thus corrosion is considered as probable when potential differentials of at least 100 mV are encountered.

On the first mapping, realized in winter time (12/01/06, 5.2°C, 70% RH, Fig. 10), potential values quite high, ranging between -69mV and -275 mV were measured. According to the ASTM standard it would indicate a low corrosion probability, but clear potential gradients were observed on the top two horizontal rebars (lines 1 and 4), and on the bottom of the testing area, indicative of a probable corrosion.

Then on the second mapping, performed in springtime (02/05/06 AM, 15.4°C, 53.3%RH, Fig. 11), even higher potential values were obtained (between -292mV and +15mV), confirming the resistivity measurement, indicating that the concrete was very dry. But on the same time, evident potential gradients were observed at the same location as in the winter measurements (i.e., on the top two horizontal rebars = lines 1 and 4, and on the bottom of the two first vertical rebars = lines c and f). Finally, the third and fourth potential maps respectively obtained after heavy wetting (02/05/06 PM, 18.5°C, 43.8% RH, Fig. 12) and heavy and repeated wetting (03/05/06 AM, 19.7°C, 54.3% RH, Fig. 13) were almost similar. The potential values drastically decreased (ranging between -20 and -367 mV) compared to the previous ones, but the same singular points were observed ; an additional one appearing more obviously on the fourth horizontal rebar (line 10).



Figures 10, 11, 12 and 13 : Potential mapping realized in winter time (12/01/06) ; and in springtime after standard moistening (02/05/06 AM), after heavy moistening (02/05/06 PM), and after heavy and repeated moistening (03/05/06 AM).

3.3. Corrosion Rate Measurements

Corrosion rate measurements were realized with a Gecor6© device, equipped with copper-copper sulfate electrodes. For each point, the values presented in this paper correspond to the average of at least three measurements, standard deviations being very low (0.01 up to 0.028).

When possible, tests were carried out on areas where, according to the potential mapping, highly probable corrosion or on the contrary no corrosion were suspected (Figs 14 and 15).

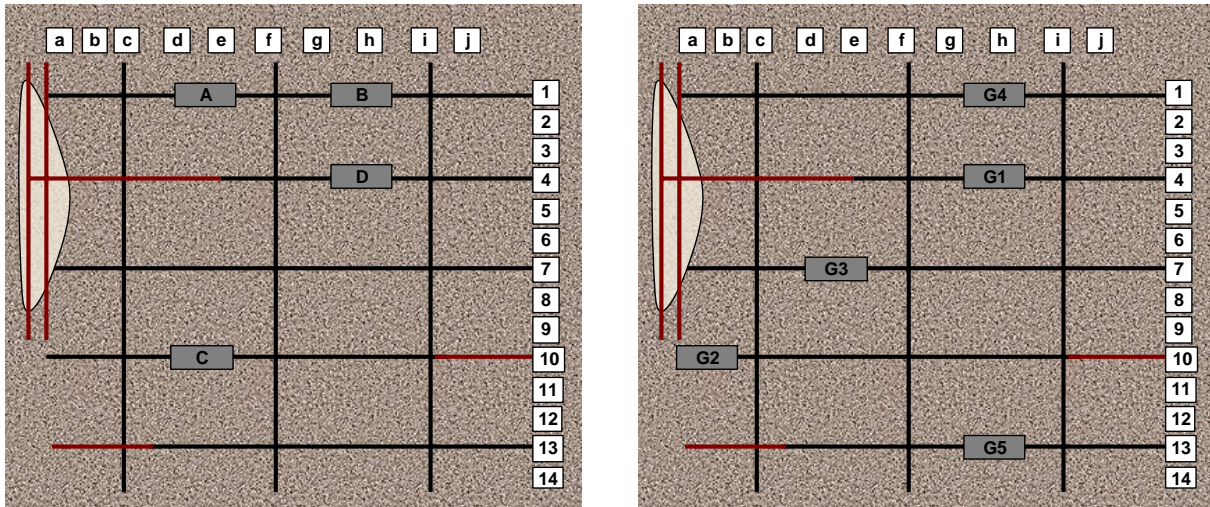
In winter time (12/01/06, 5.2°C, 70% RH, Table 1), four points were monitored, but for only three of them, exploitable data were obtained. Thus in points B and C, about 0.4 $\mu\text{A}/\text{cm}^2$ corrosion rates were measured. According to the RILEM TC 124-EMC recommendation (Table 2), in those points corrosion activity can be considered as low. When, on point A, a negligible corrosion activity was encountered (0.118 $\mu\text{A}/\text{cm}^2$). In springtime, after “standard” pre-wetting (02/05/06 AM, 15.4°C, 53.3% RH), as expected with the high resistivity and potential values previously obtained, none exploitable corrosion rate could be measured, the concrete being too dry.

After heavy moistening (02/05/06 PM, 18.5°C, 43.8% RH) and heavy and repeated moistening (03/05/06 AM, 19.7°C, 54.3% RH), two corpus of results were obtained :

- in points G2 and G5, corrosion rates almost nil were measured,

- when on points G1, G3 and G4, corrosion rates close to the low corrosion activity threshold were found.

It is interesting to notice that for both winter and spring measurements, the highest values were obtained on the same point (B or G4), where relevant potential gradients were also observed.



Figures 14 and 15 : Corrosion rate measurements location for both winter (left diagram) and spring (right diagram) measurements.

Table 1 : Corrosion rate measurements obtained in winter and spring.

Measurement Location	I _{corr} (μA/cm ²)	Potential (mV)	Date
A	0,118	-197	12/01/2006
B	0,446	-276	12/01/2006
C	0,433	-144	12/01/2006
D	/	/	12/01/2006
G1	0,167	-261	02/05/06 PM
G1b	0,192	-231	03/05/06 PM
G2	0,011	-101	02/05/06 PM
G2b	0,007	-107	03/05/06 PM
G3	0,157	-158	02/05/06 PM
G3b	0,102	-192	03/05/06 PM
G4	0,237	-359	02/05/06 PM
G4b	0,108	-275	03/05/06 PM
G5	/	/	02/05/06 PM
G5b	0,042	-191	03/05/06 PM

Table 2 : Corrosion rate thresholds of the RILEM TC 154-EMC recommendation.

Corrosion rate (μA/cm ²)	Corrosion activity
I _{corr} < 0.2	Negligible
0.2 ≤ I _{corr} ≤ 0.5	Low
0.5 < I _{corr} ≤ 1	Moderate
I _{corr} > 1	High

4 AUTOPSY

In order to validate the electrochemical measurements, six cores were sampled, notably in points prior identified as active or passive.

4.1. Phenolphthalein Test and Visual Observations

As expected, considering the visible concrete heterogeneity, confirmed by the SEM observations, wide-ranging carbonation depths (varying from none up to 4.2 cm) were measured by phenolphthalein tests (Table 3). As a consequence, as concrete covers varied from 0.7 cm, up to 1.5 cm, carbonation reached only part of the rebars.

Thus on sample O20, carbonation has reached the rebar which is visibly corroded. On the contrary, on sample O22, carbonation hardly reached the rebar which is not corroded.

Table 3 : Phenolphthalein tests and visual observations.

Core reference	Carbonation depth (cm)	Concrete cover (cm)	Rebars diameter (cm)	Visual observations
O19	2 to 4	1	0.8	Slightly corroded
O20	3 to 4,2	1.3	0.8	Corroded
O21	0.2 to 0.7	1.5	0.8	
O22	0.2 to 0.6	0.7	0.8	Non corroded
O23	0 to 0.7	x	no rebar	/
O24	0.5 to 1	x	no rebar	/

4.2. Oxide layers characterization

Two samples in which corrosion was assessed as either active (O20) or passive (O22) with the on site electrochemical measurements, were studied more in details.

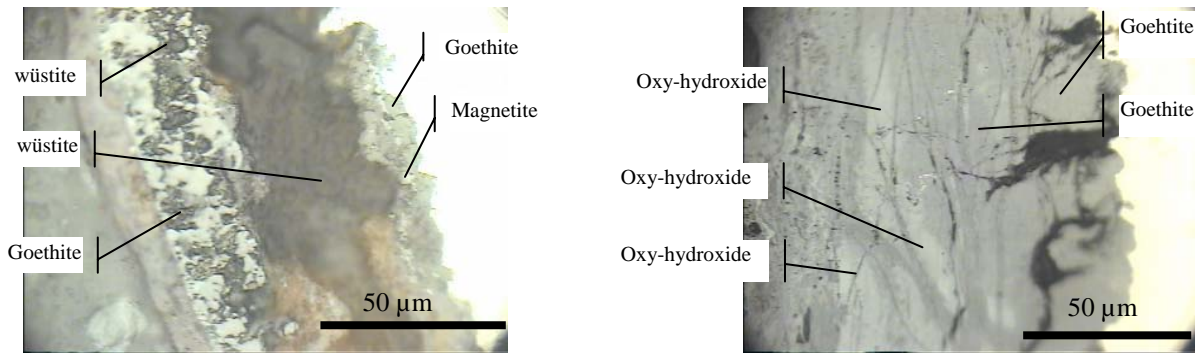
Optical microscope observation of cross sections revealed an evident difference in oxide layers thickness between the two samples. Effectively, on sample O22 a quite homogeneously thin oxides layer was observed (average maximum thickness : 50 μm , but very locally up to 100 μm), whereas on sample O20 a very heterogeneous oxide layer was encountered (thickness varying from 10 μm , up to 600 μm).

Then SEM observations coupled with EDS and Raman microspectrometry were carried out, indicating first a complexity of the corrosion layouts but also an heterogeneity of the corrosion products formed on each rebar, on a given metal section. As shown in prior studies [7], corrosion patterns can be classified into three general types depending on the oxide layer thickness and on the corrosion products identified.

It is first to be noticed that on a given metal section several types were encountered. Thus, on sample O22, type 1 pattern, called the "original layer" was predominant. It was composed of wüstite (FeO), magnetite (Fe₃O₄) and hematite (α -Fe₂O₃). These phases are characteristic of hot working at temperature above 570°C, so that they were probably formed during the manufacturing process of the rebars. But in some localized zones, a type 2 pattern was observed, goethite (α -FeOOH) being detected between the "original layer" and the metal, which is characteristic of the beginning of an active corrosion (Fig.16). These layers were about 40 μm -thick, up to 100 μm -thick in areas containing goethite.

On sample O20, two very different zones were also observed around the same rebar section. Thus type 1 was only locally detected. The major corrosion form identified was a type 3, which is very close to long-term corrosion layouts encountered on archeological samples [5]. It consisted in a thick oxide layer (up to 600 μm), mainly constituted of goethite, locally containing akaganeite (β -FeOOH), lepidocrocite (γ -FeOOH) on the external part of the corrosion layer ; and less crystallized phases appearing in lighter marblings inside the darker phases (ferrihydrite, 5Fe₂O₃.9H₂O and/or feroxyhite,

δ -FeOOH) (Fig.17). It is to be noted that at the end of a crack, a variant of this complex pattern was encountered, with traces of carbonates.



Figures 16 and 17 : Microphotographies of the corrosion layers observed on sample O22 (left picture), and on sample O20 (right picture).

5 DISCUSSION

As expected, due to the known influence of concrete moisture content on corrosion activity of the rebars, a noticeable season impact was observed on the on site electrochemical measurements, as on the same location, and after the same preconditioning, corrosion rate measurements indicated a low corrosion activity in wintertime and an absence of corrosion in springtime.

But preconditioning is also clearly of importance, as heavy preliminary moistening in springtime lead to results comparable to the wintertime ones. It is nevertheless to be noticed that heavy and repeated moistening did not improve the measurement, heavy preliminary moistening being sufficient.

Otherwise, among the electrochemical measurements performed in this study, potential mapping appeared to be the best corrosion indicator, as far as potential gradients and not absolute values were considered. Effectively, the corrosion phenomenon linked to carbonation doesn't seem to be very active, and therefore it is difficult to monitor it on site by polarization resistance measurements. Moreover, potential measurements could be performed even when the concrete was very dry, and potential gradients appeared on the same location whatever the season and the preconditioning.

Finally, an overall correct correlation was observed between the electrochemical measurements, the carbonation depths measured, and the corrosion layouts identified (Table 4). Nevertheless, quite complex patterns were observed, and as an example a noticeable impact of concrete defects such as cracks, was noticed on the nature of the corrosion products formed. This last phenomenon was already observed in prior studies [6] [7].

Table 4 : Results synthesis.

Core reference	Carbonation	Corrosion rate ($\mu\text{A}/\text{cm}^2$)	Rebars observation
O20	Yes	G1b = 0.192	Corroded, thick oxides layers
O22	No	G2b = 0.007	Almost non corroded

6 CONCLUSION

In order to try to better monitor carbonation induced corrosion on site, a series of electrochemical measurements, coupled to detailed examination of the metallic reinforcement, was performed both in winter and in springtime, on the pillars of an air purifier built in the 1950ies with reinforced concrete.

On the basis of the tests performed on this specific concrete, on site electrochemical measurements appeared very seasonal variations sensible, potential mapping being the more reliable. Moreover, as carbonation was the main mechanism involved in the rebars corrosion process, very low corrosion rates were measured. As a consequence, a diagnosis based on polarization resistance performed after

standard preconditioning in springtime would have lead to contradictory conclusions compared to a diagnosis carried out in wintertime. Nevertheless, a clear influence of preconditioning was assessed, preliminary heavy moistening clearly improving the correlation between winter and spring measurements.

Finally, the examination of the corrosion layouts, generally corroborated the on site tests. But complex patterns were observed and a noticeable impact of the concrete local defects was noted. Therefore, complementary analyses are scheduled on the same building on areas where the interpretation of the electrochemical measurements was difficult, and a new series of tests will be performed on other types of concrete.

AKNOWLEDGMENTS

The authors wish to thank the French Aerospace Lab (ONERA) team of the Meudon Center, for their kind help in this study, and the French Ministry of Culture for their financial support through the PNR program.

REFERENCES

E. Marie-Victoire, E. Cailleux, A. Texier, November 2006, Carbonation and historical buildings made of concrete, *Journal de physique IV*, vol. 136, p. 305-318.

ASTM standards, 04.02 concrete and aggregates, C876, Standard test method for half cell potentials of uncoated reinforcing steel in concrete. .

B. Elsener & Al., 2003, Half-cell potential measurements – Potential mapping on reinforced concrete structures, RILEM TC 154-EMC : *Electrochemical Techniques for Measuring Metallic Corrosion - Recommendations, Materials and Structures*, Vol. 36, pp.461-471.

C. Andrade, A. Alonso & Al., 2004, Test method for on-site corrosion rate measurement of steel reinforcement in concrete by means of the polarization resistance method. RILEM TC 154-EMC : *Electrochemical Techniques for Measuring Metallic Corrosion - Recommendations, Materials and Structures*, Vol. 37, pp.623-643.

W-J. Chitty, P. Dillmann, V. L'Hostis, G. Béranger, 2005. Use of ferrous archaeological artefacts in binders to improve the knowledge on long term corrosion mechanisms of reinforced concrete, Eurocorr'05, Lisbon, Portugal, September

V. l'Hostis, L. Vincent, V. Praca, D. Neff, L. Bellot-Gurlet, P. Dillmann, 2007. Characterization of long-term corrosion of rebars embedded in concretes from French historical buildings aged from 50 to 80 years, Eurocorr'07, Freiburg im Breisgau, Germany, 9-13 September

D. Neff, E. Marie-Victoire, V. l'Hostis, E. Cailleux, L. Vincent, A., L. Bellot-Gurlet, P. Dillmann, 2007. Preservation of historical buildings : understanding of corrosion mechanisms of metallic rebars in concrete, Metal 07 : *Study and conservation of composite artefacts, meeting of the ICOM-CC Metal WG*, Amsterdam, 17-21 September

Neff, D., L. Bellot-Gurlet & al., 2006. Raman imaging of ancient rust scales on archaeological iron artefacts for long term atmospheric corrosion mechanisms study, *Journal of Raman Spectroscopy* 37, pp.1228-1237,

dbmc

11th International Conference on
Durability of Building Materials and Components

Durability of Building Materials and Components 11

Globality and Locality in Durability

Proceedings CD of the Eleventh International Conference
on Durability of Building Materials and Components, 11dbmc

Istanbul, Turkey
11-14 May 2008

Editors:

A. Nil Türkeri

I.T.U. Faculty of Architecture

Özkan Şengül

I.T.U. Faculty of Civil Engineering



dbmc

11th International Conference on
Durability of Building Materials and Components

All rights reserved. No part of this publication may be reproduced, stored in a retrieval system, or transmitted in any form or by any other means, electronic, mechanical photocopying, recording or otherwise, without prior written permission of Istanbul Technical University, Istanbul, Turkey.

Full Proceedings CD
ISBN: 978-975-561-330-7

Published in book form as well:
Durability of Building Materials and Components 11: Proceedings of the Eleventh International Conference on Durability of Building Materials and Components
Complete in 4 volumes
ISBN: 978-975-561-325-3 (set number)

Correct citation: Türkeri, A. Nil and Şengül, Özkan (*Editors*) 2008. Durability of Building Materials and Components 11: *Globality and Locality in Durability*. CD-ROM.

